Original Contribution

Defining the Ischemic Penumbra Using Magnetic Resonance Oxygen Metabolic Index

Hongyu An, DSc*; Andria L. Ford, MD*; Yasheng Chen, PhD; Hongtu Zhu, PhD; Rosana Ponisio, MD; Gyanendra Kumar, MD; Amirali Modir Shanechi, MD; Naim Khoury, MD; Katie D. Vo, MD; Jennifer Williams, RN; Colin P. Derdeyn, MD; Michael N. Diringer, MD; Peter Panagos, MD; William J. Powers, MD; Jin-Moo Lee, MD, PhD†; Weili Lin, PhD†

Background and Purpose—Penumbral biomarkers promise to individualize treatment windows in acute ischemic stroke. We used a novel magnetic resonance imaging approach that measures oxygen metabolic index (OMI), a parameter closely related to positron emission tomography–derived cerebral metabolic rate of oxygen utilization ($CMRO_2$), to derive a pair of ischemic thresholds: (1) an irreversible-injury threshold that differentiates ischemic core from penumbra and (2) a reversible-injury threshold that differentiates penumbra from tissue not-at-risk for infarction.

Methods—Forty patients with acute ischemic stroke underwent magnetic resonance imaging at 3 time points after stroke onset: <4.5 hours (for OMI threshold derivation), 6 hours (to determine reperfusion status), and 1 month (for infarct probability determination). A dynamic susceptibility contrast method measured cerebral blood flow, and an asymmetrical spin echo sequence measured oxygen extraction fraction, to derive OMI (OMI=cerebral blood flow×oxygen extraction fraction). Putative ischemic threshold pairs were iteratively tested using a computation-intensive method to derive infarct probabilities in 3 tissue groups defined by the thresholds (core, penumbra, and not-at-risk tissue). An optimal threshold pair was chosen based on its ability to predict infarction in the core, reperfusion-dependent survival in the penumbra, and survival in not-at-risk tissue. The predictive abilities of the thresholds were then tested within the same cohort using a 10-fold cross-validation method.

Results—The optimal OMI ischemic thresholds were found to be 0.28 and 0.42 of normal values in the contralateral hemisphere. Using the 10-fold cross-validation method, median infarct probabilities were 90.6% for core, 89.7% for nonreperfused penumbra, 9.95% for reperfused penumbra, and 6.28% for not-at-risk tissue.

Conclusions—OMI thresholds, derived using voxel-based, reperfusion-dependent infarct probabilities, delineated the ischemic penumbra with high predictive ability. These thresholds will require confirmation in an independent patient sample. **(*Stroke*. 2015;46:00-00. DOI: 10.1161/STROKEAHA.114.008154.)**

Key Words: magnetic resonance imaging ■ reperfusion

Background and Purpose

Imaging the ischemic penumbra during hyperacute stroke has been actively investigated because of its potential to individualize therapeutic opportunities beyond population-defined time-windows. The ischemic penumbra was defined by Astrup[1] as a zone of nonfunctioning but viable tissue that may recover its function if blood flow can be restored, for example, by therapeutic intervention. This concept originated from electrophysiological studies in primates, which revealed 2 cerebral blood flow (CBF) thresholds: a lower threshold of ion-pump failure that was associated with tissue infarction, and an upper threshold denoted by electric failure, but was associated with preserved tissue structure. The initial use of CBF thresholds to define the penumbra was problematic because the threshold delineating the ischemic core changed with increasing duration of ischemia.[2] Subsequent positron emission tomography (PET) studies in animal models and in patients with stroke demonstrated that as CBF dropped in the affected region, oxygen extraction fraction (OEF) increased in attempt to maintain tissue-level metabolism or cerebral metabolic rate of oxygen utilization ($CMRO_2$=CBF×OEF×arterial oxygen content). Despite elevation of OEF in the peri-infarct

Received November 18, 2014; final revision received January 28, 2015; accepted January 28, 2015.

From the Biomedical Research Imaging Center and Departments of Radiology (H.A., Y.C., W.L.), Biostatistics (H.Z.), and Department of Neurology (W.J.P., W.L.), University of North Carolina at Chapel Hill; Department of Neurology (A.L.F., G.K., N.K., J.-M.L.), Department of Radiology (R.P., K.D.V., C.P.D., J.-M.L.), Department of Emergency Medicine (P.P.), and School of Medicine (A.L.F., G.K., N.K., J.-M.L., R.P., K.D.V., C.P.D., J.-M.L., A.M.S., P.P.), Washington University, St. Louis, MO; and Emergency Department, Barnes-Jewish Hospital, St. Louis, MO (J.W.).

*Drs An and Ford contributed equally.

†Drs Lee and Lin are joint senior authors.

The online-only Data Supplement is available with this article at http://stroke.ahajournals.org/lookup/suppl/doi:10.1161/STROKEAHA.114.008154/-/DC1.

Correspondence to Weili Lin, PhD, University of North Carolina, 125 Mason Farm Rd, Campus Box 7515, Chapel Hill, NC 27599, E-mail weili_lin@med.unc.edu or Jin-Moo Lee, MD, PhD, Department of Neurology, Washington University, School of Medicine, 660 South Euclid Ave, Campus Box 8111, St. Louis, MO 63110, E-mail leejm@neuro.wustl.edu

region, OEF alone was found to be a relatively weak predictor of tissue outcome,[3] whereas $CMRO_2$ more consistently delineated tissue that eventually died[4–6] with thresholds for infarction ranging from 0.87 to 1.7 mL 100 g^{-1} min^{-1} $CMRO_2$ (<23% to 55% of normal values). Values at the lower end of the range were derived from single voxel measurements of both gray and white matter, whereas those at the higher end were determined from larger regions of interest primarily in gray matter.[4,7–11] Unlike CBF thresholds, $CMRO_2$ thresholds seemed independent of the time interval after stroke onset, making them ideal for imaging salvageable tissue in patients with stroke who present at various times after stroke onset.[12]

Given the logistical hurdles of PET in patients with hyperacute stroke, magnetic resonance (MR) and computed tomographic methods have been actively explored. Although initial studies of MR diffusion perfusion mismatch (DPM) and computed tomographic perfusion mismatch as a penumbral imaging signature were promising, clinical trials were unable to demonstrate improved clinical outcomes when selecting patients with DPM for therapy. The Echoplanar Imaging Thrombolytic Evaluation Trial (EPITHET) randomized patients to tissue-type plasminogen activator (tPA) versus placebo between 3 and 6 hours from stroke onset.[13] Patients with DPM who were given tPA did not show significantly decreased infarct growth when compared with those given placebo. The Desmoteplase in Acute Stroke (DIAS)-II trial did not demonstrate any benefit with a novel thrombolytic, desmoteplase, compared with placebo in mismatch-selected patients.[14] Mechanical Retrieval and Recanalization of Stroke Clots Using Embolectomy (MR-RESCUE) randomized patients to clot retrieval versus medical therapy within 8 hours of onset and found no benefit from intervention in patients with penumbral pattern using mismatch criteria.[15] Further DPM trials are underway to determine whether optimized DPM thresholds will identify individuals who might benefit from acute interventions.

With the goal of finding a physiological biomarker of penumbral tissue, we developed an MR method capable of assessing cerebral oxygen metabolism termed MR-oxygen metabolic index (OMI).[16] This method has been validated in animal models subjected to hypoxia, hypercapnia, and middle cerebral artery occlusion against jugular venous oxygen saturation sampling.[17] In healthy subjects inhaling variable mixtures of carbogen, OMI yielded similar values to those found in PET studies with high reproducibility.[18] Furthermore, in a study of patients with acute stroke, OMI values in the eventually infarcted region were 0.40±0.24 of the contralateral hemisphere, consistent with PET-derived $CMRO_2$ values for nonviable tissue.[8]

In this prospective imaging study, we tested OMI as a predictor of tissue fate in a cohort of patients with acute ischemic stroke imaged within 4.5 hours of stroke symptom onset and reimaged at 6 hours after stroke onset to assess reperfusion status. Using a voxel-by-voxel approach, our aim was to derive 2 quantitative ischemic thresholds for delineation of the ischemic penumbra: (1) a lower threshold of irreversible-injury, which differentiated ischemic core from penumbra and (2) an upper threshold of reversible injury, which differentiated penumbra from oligemia. Consistent with Astrup's definition,[1] penumbra was defined based on reperfusion-dependent tissue survival: if reperfused, penumbral tissue should survive; if not reperfused, penumbral tissue should die.

Methods

Patients and Inclusion Criteria

Approval of the protocol was obtained from the Washington University Human Studies Committee. This was a prospective, observational magnetic resonance imaging study in patients with acute ischemic stroke at a large, urban, tertiary care referral center. There was no overlap of patients between the current study and previous reports of OMI. After providing written informed consent, both intravenous tPA-treated and untreated patients with acute ischemic stroke with a National Institutes of Health Stroke Scale ≥5 were enrolled (full inclusion and exclusion criteria are available in Table I in the online-only Data Supplement). The study imposed no delay in time-to-tPA treatment and no deviation from standard monitoring practices. The National Institutes of Health Stroke Scale was collected prospectively by a stroke neurologist or stroke research coordinator on admission, at 72 hours, and at all imaging time points (tp). Clinical data including demographic data and medical history were obtained by the research coordinator prospectively at the time of patient enrollment.

Magnetic Resonance Imaging Protocol

Patients underwent serial Magnetic Resonance Imaging scans at 3 tp: within 4.5 hours (tp1), at 6 hours (tp2), and at 1 month (tp3) after stroke onset, on a 3T Siemens whole body Trio. For patients receiving intravenous tPA, the tp1 scan was performed as soon as possible after tPA bolus (during tPA infusion). Six hours was chosen for the time of reperfusion measurement because reperfusion-based therapies administered within, but not beyond, this time-frame have demonstrated clinical efficacy.[19,20] One month was chosen as the time for final infarct determination because stroke-related edema has diminished significantly by 1 month and atrophy may become significant beyond 1 month.[21,22]

The protocol included diffusion-weighted, fluid-attenuated inversion recovery (repetition time/echo time=10000/115 ms; inversion time=2500 ms; matrix=512×416; 20 slices, slice thickness=5 mm), magnetization prepared rapid azquisition gradient echo, and dynamic susceptibility contrast perfusion images with 0.2 mL/kg gadolinium contrast injected at 5 mL/s (a T2*-weighted gradient echo echoplanar imaging sequence; repetition time/echo time=1500/43 ms; 14 slices, slice thickness=5 mm, zero interslice gap; matrix=128×128). The protocol did not include magnetic resonance angiography. The dynamic susceptibility contrast method provided the perfusion-weighted imaging for calculation of CBF and cerebral blood volume maps. Mean transit time (MTT) was calculated as cerebral blood volume/CBF. Voxels within the proximal middle cerebral artery of the contralateral hemisphere were manually chosen, and the mean concentration curve of these voxels was used as the arterial input function. A time-shift insensitive block-circulant singular value decomposition method was used to minimize effects of time lag of the arterial input function on perfusion measurements.[23] To minimize large-vessel effects, which contribute to artifactually high signal near the cortical vertices, voxels with cerebral blood volume of >10% were removed and excluded from further analysis in deriving OMI thresholds for core, penumbra, and not-at-risk tissues (normal cerebral blood volume for gray matter is 3%–5% and for white matter is 1.5%–3%). An asymmetrical spin echo sequence was used to calculate OEF.[24] OMI was calculated as CBF×OEF. Measurements were normalized to the contralateral unaffected hemisphere. Detailed descriptions for quantification of OEF and OMI can be found elsewhere.[24,25] MR-OEF images were acquired in 30 s epochs, so that those with significant motion artifact could be removed from the final signal-averaged OEF measure. If >30% of OEF images from a single tp were removed because of motion, the patient was removed from the analysis.

Six-parameter rigid image registration was performed to align all images across tp1, tp2, and tp3 for each patient using a well-established linear registration tool FSL 3.2 (FMRIB, Oxford, United

Kingdom).[26] Accuracy of image registration was evaluated manually by a board-certified neuroradiologist (K.D.V.) who checked several structural landmarks, such as the ventricle and brain boundaries, in all registered images and their corresponding template image for each patient. If coregistration was found to be discrepant from the template image of >3 voxels in any direction, the registration algorithm was modified and rerun to improve alignment. Using this manual checking process, no patients who had all 3 imaging tp were removed because of inadequate coregistration.

Tissue segmentation into gray and white matter, necessary for calculation of CBF and OMI before normalization with the contralateral hemisphere, was performed using a semiautomated approach using FSL 3.2 (FMRIB) for automatic segmentation[26] followed by manual correction by a board-certified neuroradiologist (M.R.P.) using SNAP-ITK 2.2.0.[27] For delineation of the final infarct, hyperintense lesions were manually outlined on the 1-month fluid-attenuated inversion recovery image by a board-certified vascular neurologist (A.L.F.) who was blinded to the OMI data. Each voxel on the 1-month fluid-attenuated inversion recovery image was assigned a value of dead or alive for infarct probability (IP) analysis.

Derivation of OMI Thresholds

All tp1 OMI voxels within the affected hemisphere were included for OMI threshold evaluation. Two OMI thresholds for delineating the ischemic penumbra were derived from the individual patient tp1 OMI maps based on a computation-intensive approach searching for the optimal threshold pair, which included (1) a lower irreversible-injury OMI threshold to distinguish the ischemic core from the ischemic penumbra and (2) an upper reversible injury OMI threshold to distinguish ischemic penumbra from tissue not-at-risk for infarction. Specifically, a 4-cell approach, reflecting 4 different tissue categories (core, nonreperfused penumbra, reperfused penumbra, and not-as-risk tissue) was used. OMI threshold pairs were iteratively tested, searching for the threshold pair, which resulted in IP closest to ideal values in each tissue group of interest: (1) core (tissue died regardless of reperfusion), ideal IP=100%; (2) nonreperfused_penumbra (tissue died without reperfusion), ideal IP=100%; (3) reperfused_penumbra (tissue survived with reperfusion), ideal IP=0%; and (4) not-as-risk tissue (tissue survived regardless of reperfusion), ideal IP=0% (Figure 1). To this end, the threshold pair with the lowest average prediction error, a metric averaging the differences for each tissue group's actual IP from the ideal was selected as optimal pair for delineating the penumbra. Therefore, average prediction error=($|100\%-IP_{core}|+|100\%-IP_{nonreperfused\_penumbra}|+|0\%-IP_{reperfused\_penumbra}|+|0\%-IP_{not\text{-}at\text{-}risk}|$)/4. Threshold pairs were derived in individual patients, and the median IP and corresponding average prediction error were calculated for each pair. The pair with the lowest median average prediction error across the total sample was chosen as optimal. Hypoperfusion was defined in regions with MTT prolongation beyond the median MTT of the contralateral hemisphere (MTTp) >4 s at tp1. Reperfusion within the penumbra was defined as MTTp<4 s at tp2 based on our previous analyses evaluating MTTp thresholds.[28] Nonreperfusion was defined as a voxel with an MTTp perfusion deficit >4 s at tp2. OMI threshold ranges (0.16–0.32 for irreversible-injury and 0.38–0.52 for reversible-injury in increments of 0.02) were chosen based on threshold ranges found within PET literature measuring $CMRO_2$ in patients with ischemic stroke.[29] To reduce noise-induced effects, a minimum volume of 1 mL for a tissue group was required to be included for average prediction error calculation.

Cross-Validation of OMI Thresholds

The predictive abilities of the derived OMI thresholds were tested in the same sample using a 10-fold cross-validation method.[30] The sample was partitioned into 10 equal subsamples. Of the 10 subsamples, 9 subsamples were used to derive the optimal ischemic thresholds. The derived thresholds were then tested on each of the patients within the 1 subsample left-out; average prediction error and the IP for the tissue groups were calculated. This cross-validation process was repeated 9×, with each of the 10 subsamples used only once as the test subsample. Population-level IP and average prediction errors were displayed as median [25th quartile, 75th quartile]. Analyses were performed using Matlab version R2012a.

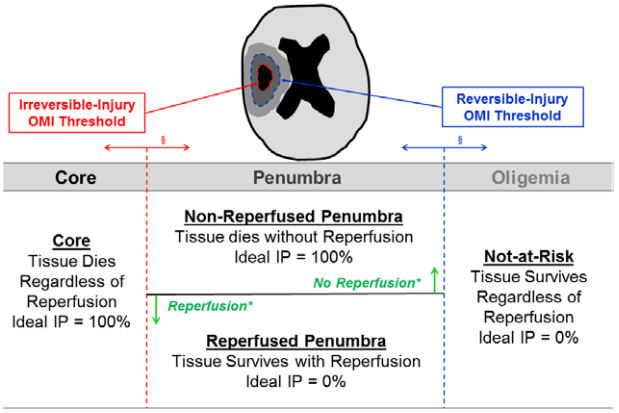

Figure 1. Deriving oxygen metabolic index (OMI) penumbral thresholds. (§) Irreversible-injury and reversible-injury OMI threshold pairs separated the tissue within the ischemic hemisphere into core, penumbra, and not-at-risk; penumbra was further subdivided by reperfusion status (nonreperfused penumbra and reperfused penumbra). For each pair, the infarct probability (IP) from each tissue group was calculated. A computation-intensive search method was performed to find the OMI threshold pair that corresponded to the lowest average prediction error (a metric averaging the differences of the actual infarct probabilities from ideal infarct probabilities for all tissue groups). Average prediction error (APE)=($|100\%-IP_{core}|+|100\%-IP_{nonreperfused\_penumbra}|+|0\%-IP_{reperfused\_penumbra}|+|0\%-IP_{not\text{-}at\text{-}risk}|$)/4; ideal APE=0%. Pairs of irreversible and reversible-injury thresholds were iteratively tested, and infarct probabilities in each of the 4 tissue groups and the corresponding average prediction error were calculated. The threshold pair with the lowest average prediction error was selected as the pair of optimal OMI thresholds.

Results

Sixty-four patients who met all inclusion and exclusion criteria were consented and underwent tp1 imaging, of whom 24 patients were excluded because of (1) inability to get tp2 because of medical instability, intolerance of tp1 magnetic resonance imaging because of claustrophobia, or early reperfusion on tp1 imaging (n=7); (2) lost to follow-up or died before last imaging session (n=10); or (3) poor data quality because of motion artifact (n=7; Figure I in the online-only Data Supplement). Therefore, 40 patients were included in the final analysis. Baseline clinical and imaging characteristics for the 40 patients are shown in Table 1. These patients were imaged at a median of 2.7 hours (tp1), 6.3 hours (tp2), and 1 month (tp3) after stroke onset.

Deriving the Optimal OMI Thresholds for Delineating the Penumbra

Putative OMI threshold pairs were used to define 3 tissue groups: core, penumbra, and not-at-risk. The putative penumbra was further subdivided by reperfusion status (nonreperfused penumbra and reperfused penumbra). Infarct probabilities were determined for each of these 4 tissue groups: core, nonreperfused penumbra, reperfused penumbra, and not-at-risk. Figure 2 shows an example from 1 patient, using the OMI threshold pair, 0.28 for irreversible-injury and 0.42 for reversible injury. IP for this patient were 98.0% for core, 68.3% for nonreperfused penumbra, 9.8% for reperfused

Table 1. Patient Characteristics (n=40)

Women, n (%)	14 (35%)
Age, y	64 [57, 72]
Admission NIHSS	14 [8, 19]
Black, n (%)	14 (35%)
tPA treatment, n (%)	30 (75%)
Admission mean arterial pressure, mm Hg	114 [106, 128]
Admission glucose, mg/dL	126 [107, 149]
Time to tp1, h	2.7 [2.1, 3.5]
Time to tp2, h	6.3 [6.1, 6.5]
History of hypertension, n (%)	31 (78%)
History of diabetes mellitus, n (%)	11 (28%)
History of congestive heart failure, n (%)	5 (12%)
Current tobacco use, n (%)	12 (30%)
History of coronary artery disease, n (%)	12 (30%)
History of stroke or TIA, n (%)	8 (20%)

Continuous data shown as median [interquartile range]. NIHSS indicates National Institutes of Health Stroke Scale; TIA, transient ischemic attack; tp1, time point 1 magnetic resonance imaging and tp2, time point 2 magnetic resonance imaging.

penumbra, and 1.1% for not-at-risk, yielding an average prediction error of 11.2%. The average prediction error is a value that describes the average deviation from ideal IP (see Methods section of this article).

Using a computation-intensive search method, all possible threshold pairs within predefined ranges were applied to all patients, and IP was calculated for each of the tissue groups. A median population average prediction error was calculated for each threshold pair. A matrix of threshold pairs with its corresponding median average prediction error values was created and displayed as a 3-dimensional graph (Figure 3). The ideal threshold pair was defined as the pair with the lowest average prediction error value, indicating the lowest deviation from ideal prediction of tissue outcome. A single threshold pair was found to have the lowest average prediction error from the patient population, corresponding to an OMI threshold of 0.28 for irreversible-injury and 0.42 for reversible injury (Figure 3, *). This optimal threshold pair yielded an average prediction error of 8.75%, corresponding to the following IPs: (1) 92.9% (61.5, 97.6) for core, 92.2% (77.3, 96.4) for nonreperfused penumbra, 9.95% (0.30, 28.5) for reperfused penumbra, and 6.28% (1.72, 14.0) for not-at-risk tissue.

Testing the Predictive Ability of OMI Thresholds

The 10-fold cross-validation method produced thresholds ranging from 0.24 to 0.28 for the irreversible-injury threshold and from 0.42 to 0.44 for the reversible injury threshold for the 10 subsample derivation sets. The 10 subsample threshold data are shown in Table 2. The median IPs in the 10 subsample test sets were 90.6% (61.5, 97.7) for core, 89.7% (78.0, 95.2) for nonreperfused penumbra, 9.95% (0.33, 28.2) for reperfused penumbra, and 6.28% (1.72, 14.0) for not-at-risk tissue, corresponding to an average prediction error of 11.4% (2.69, 21.0; Table 3).

Table 3. OMI Threshold 10-Fold Cross-Validation: Population-Derived Median Infarct Probabilities and Average Prediction Error

	Core IP	Penumbra IPs	Not-at-Risk IP
Nonreperfusion	90.6% [61.5, 97.7]	89.7% [78.0, 95.2]	6.28% [1.72, 14.0]
Reperfusion		9.95% [0.33, 28.2]	
APE*=11.4% [2.69, 21.0]			

Data shown as median [25th quartile, 75th quartile]. APE indicates average prediction error; IP, infarct probability; and OMI, oxygen metabolic index.

*APE (average prediction error)=(|100%−IP_{core}|+|100%−$IP_{non\text{-}reperfused\_penumbra}$|+|0%−$IP_{reperfused\_penumbra}$|+|0%−$IP_{not\text{-}at\text{-}risk}$|)/4; ideal APE=0%.

Discussion

In this prospective imaging study, a novel MR parameter designed to measure cerebral OMI was tested to determine whether it could accurately delineate the ischemic penumbra. Two optimal OMI thresholds were identified which delineated core, penumbra, and not-at-risk tissue and yielded reperfusion-dependent IP close to ideal predicted tissue fate. Penumbral IPs within each voxel of tissue were strictly defined by reperfusion status: the ideal IPs was 0% if reperfused and 100% if not reperfused. Moreover, when the optimal thresholds were

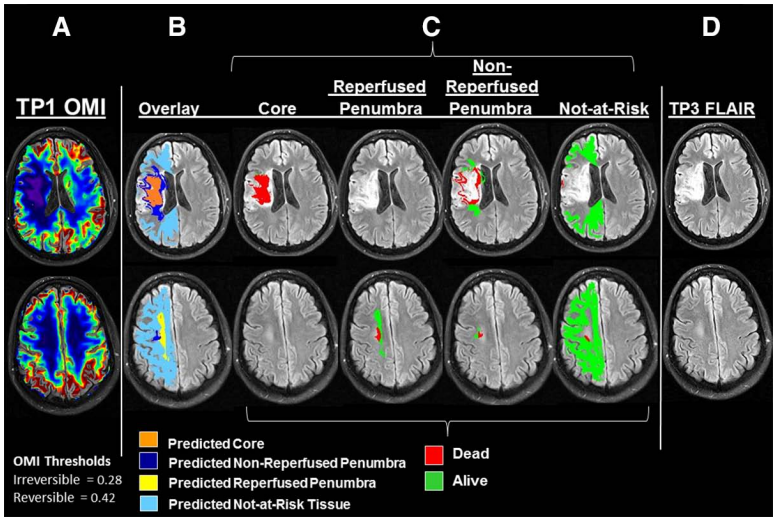

Figure 2. Patient example. A 27-year-old man with a right middle cerebral artery stroke (National Institutes of Health Stroke Scale=16) underwent time point (tp) 1 magnetic resonance imaging at 2:10 after symptom onset (during tissue-type plasminogen activator infusion) followed by tp2 magnetic resonance imaging at 6:28 after onset. Using tp1 oxygen metabolic index (OMI) map (column **A**), an example OMI threshold pair (core/penumbra=0.28, penumbra/not-at-risk=0.42) divided the tissue into predicted core, penumbra, and not-at-risk; penumbra was further subdivided based on reperfusion status (determined by tp2 scan; column **B**). For each of the 4 tissue groups (**C**), tissue that died (red) or survived (green) was determined based on the infarct delineated on fluid-attenuated inversion recovery imaging at 1 month (column **D**). The actual infarct probabilities from each group were calculated and subtracted from the ideal infarct probabilities, from which the average prediction error for this threshold pair in this patient was calculated.

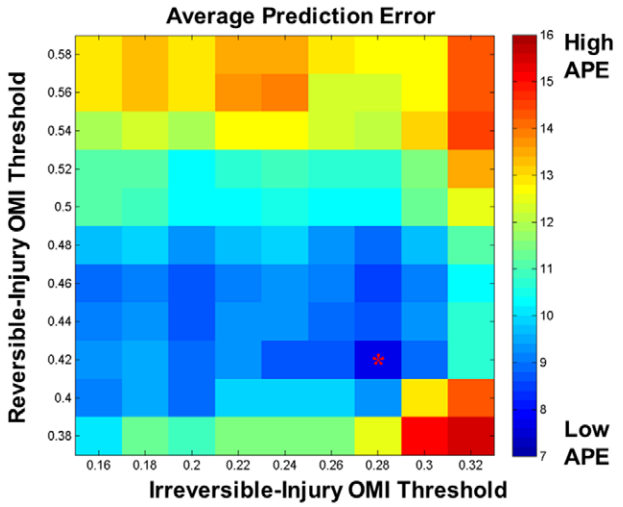

Figure 3. Population-derived average prediction errors (APE) as a function of varying the oxygen metabolic index (OMI) core/penumbra and penumbra/not-at-risk threshold pairs. A 3-dimensional matrix of OMI threshold pairs with the corresponding median APE values was plotted. The irreversible injury OMI threshold is on the *x*-axis. The reversible injury OMI threshold is on the *y*-axis. The APE is on the color scale (in-plane) axis with cool colors representing the lowest average prediction error (closest to ideal) and warm colors representing the highest average prediction error (farthest from ideal). The ideal threshold pair was defined as the pair with the lowest average prediction error value, indicating the lowest deviation from ideal tissue outcome. The lowest single minimum average prediction error (8.75%) is found at the dark-blue square (*) corresponding to an irreversible injury threshold of 0.28 and a reversible injury threshold of 0.42.

tested using the cross-validation technique, thresholds demonstrated little variability and yielded median IPs that were near ideal, suggesting that the derived thresholds were highly predictive of ideal tissue fate across the population.

The current study has several strengths: (1) our definition of penumbra was based on the definition by Astrup,[1] as operationalized by others,[5] requiring that reperfused voxels between the 2 optimal thresholds have low IP and nonreperfused voxels have high IP; (2) the timing of reperfusion measurement at 6 hours was chosen specifically to be within a time window known to affect clinical outcome in previous stroke populations[19,31]; we aimed to define the OMI thresholds

Table 2. Cross-Validation Results for the Optimal OMI Thresholds in the 10 Subsamples

Subsample	Irreversible-Injury OMI Threshold	Reversible-Injury OMI Threshold
1	0.28	0.42
2	0.28	0.42
3	0.28	0.42
4	0.24	0.42
5	0.28	0.42
6	0.28	0.42
7	0.28	0.42
8	0.28	0.42
9	0.26	0.44
10	0.28	0.42

OMI indicates oxygen metabolic index.

Table 3. Oxygen Metabolic Index Threshold 10-Fold Cross-Validation: Population-Derived Median IPs and APE

	Core IP	Penumbra IPs	Not-at-Risk IP
Nonreperfusion	90.6% [61.5, 97.7]	89.7% [78.0, 95.2]	6.28% [1.72, 14.0]
Reperfusion		9.95% [0.33, 28.2]	
APE*=11.4% [2.69, 21.0]			

Data shown as median [25th quartile, 75th quartile]. APE indicates average prediction error; and IP, infarct probability.

*APE= $|100\%-IP_{core}|+|100\%-IP_{nonreperfused\_penumbra}|+|0\%-IP_{reperfused\_penumbra}|+|0\%-IP_{not\text{-}at\text{-}risk}|)/4$; ideal APE=0%.

based on clinically relevant reperfusion that would truly salvage tissue[28]; (3) we used a novel, unbiased approach to derive ischemic thresholds using a computation-intensive search method to minimize average prediction error; and (4) a voxel-wise approach was used for all analyses: all definitions were applied to coregistered voxels at 3 time points, rather than visual, regional, or volumetric analyses.[13,14,32]

In the current study, we derived OMI thresholds for a time window in which reperfusion-promoting therapies are known to improve outcomes; however, additional studies will test these thresholds at later windows. PET data suggest that the $CMRO_2$ threshold delineating tissue outcome may be independent of time from symptom onset.[12,29] This theory of time-independence is based on independent studies, which have measured $CMRO_2$ at different tp and arrived at a similar threshold for delineating tissue with eventual infarction; however, this threshold has not been tested for time-independence within a single study. Therefore, it will be important to determine whether the OMI thresholds derived in this study will predict reperfusion-based tissue fate at later time windows.

A challenge with clinical trials to date has been defining penumbral thresholds, which have largely been chosen empirically.[13,14,33] In early DPM trials, the reversible injury threshold (using a perfusion-weighted imaging–based parameter to separate penumbra from oligemia) was found to encompass significant oligemic tissue that was not at true risk for eventual infarction.[13,33] Post hoc analyses helped to refine the optimal thresholds for use in subsequent studies.[15,34–36] More recently, MR-RESCUE investigators rigorously derived the threshold for irreversibly-injury by developing a multiparametric model (including diffusion-weighted imaging and perfusion-weighted imaging parameters) to predict the infarct core in the setting of successful recanalization.[37] The threshold for reversible injury was not optimized but was empirically chosen. To build on these methods, we aimed to prospectively identify the best-performing, quantitative penumbral thresholds for both irreversible- and reversible-injury so that the optimal thresholds would be known if tested within the context of a clinical trial.

This study has several limitations. (1) Data were obtained from a single institution; therefore, the generalizability of thresholds to other populations is unknown. (2) Inclusion criteria required National Institutes of Health Stroke Scale ≥5; therefore, this cohort captured strokes of greater severity (median National Institutes of Health Stroke Scale=14) than average patients with stroke. 3) Because the first imaging session occurred, on average, 46 minutes after tPA treatment, some tissue that was initially ischemic might have been lost to analysis because of

early reperfusion. (4) Tissue (gray-white matter) segmentation is required for calculating normalized OMI. Therefore, before implementation in clinical practice, a rapid processing algorithm will need to be developed, similar to current rapid postprocessing tools used for diffusion perfusion mismatch.[38] (5) We assessed the reproducibility and predictive ability of the OMI thresholds on the same patient cohort in which the thresholds were derived using a statistical resampling method. Therefore, the thresholds will need to be tested in an independent population. (6) The clinical use of OMI ischemic thresholds will need to be tested to evaluate how much OMI-defined penumbral tissue is required to yield meaningful clinical benefit and whether OMI promotes the efficacy of an intervention by appropriately selecting patients for therapy. (7) Finally, we are directly comparing MR-OMI values to PET-derived $CMRO_2$ values in patients with cerebrovascular disease in an ongoing study, which will permit further refinement of MR-OMI.

Conclusions

OMI ischemic thresholds, derived using voxel-based final infarct and reperfusion status, delineated the ischemic penumbra with high predictive ability and were consistent when retested within the population. These thresholds will require further testing in independent patient cohorts.

Acknowledgments

We are grateful to the stroke research coordinators and emergency department staff for the help with patient enrollment.

Sources of Funding

This study was supported by grants from National Institute of Health (NIH) 5P50NS055977 (to Dr Lee, Dr Derdeyn, Dr Powers, W. Lin, and H. An) and K23 NS069807 (to Dr Ford) and from the Washington University Institute of Clinical and Translational Sciences grant UL1 TR000448 from the National Center for Advancing Translational Sciences of the National Institutes of Health.

Disclosures

H. An and W. Lin receive research support from Siemens. Colin Derdeyn receives modest consulting fees from Penumbra, Inc. and MicroVention. Dr Powers received honoraria for 2 invited continuing medical education stroke lectures. The other authors reports no conflicts.

References

1. Astrup J. Energy-requiring cell functions in the ischemic brain. Their critical supply and possible inhibition in protective therapy. *J Neurosurg*. 1982;56:482–497. doi: 10.3171/jns.1982.56.4.0482.
2. Jones TH, Morawetz RB, Crowell RM, Marcoux FW, FitzGibbon SJ, DeGirolami U, et al. Thresholds of focal cerebral ischemia in awake monkeys. *J Neurosurg*. 1981;54:773–782. doi: 10.3171/jns.1981.54.6.0773.
3. Young AR, Sette G, Touzani O, Rioux P, Derlon JM, MacKenzie ET, et al. Relationships between high oxygen extraction fraction in the acute stage and final infarction in reversible middle cerebral artery occlusion: an investigation in anesthetized baboons with positron emission tomography. *J Cereb Blood Flow Metab*. 1996;16:1176–1188. doi: 10.1097/00004647-199611000-00012.
4. Heiss WD, Huber M, Fink GR, Herholz K, Pietrzyk U, Wagner R, et al. Progressive derangement of periinfarct viable tissue in ischemic stroke. *J Cereb Blood Flow Metab*. 1992;12:193–203. doi: 10.1038/jcbfm.1992.29.
5. Furlan M, Marchal G, Viader F, Derlon JM, Baron JC. Spontaneous neurological recovery after stroke and the fate of the ischemic penumbra. *Ann Neurol*. 1996;40:216–226. doi: 10.1002/ana.410400213.
6. Wise RJ, Bernardi S, Frackowiak RS, Legg NJ, Jones T. Serial observations on the pathophysiology of acute stroke. The transition from ischaemia to infarction as reflected in regional oxygen extraction. *Brain*. 1983;106 (Pt 1):197–222.
7. Giffard C, Young AR, Kerrouche N, Derlon JM, Baron JC. Outcome of acutely ischemic brain tissue in prolonged middle cerebral artery occlusion: a serial positron emission tomography investigation in the baboon. *J Cereb Blood Flow Metab*. 2004;24:495–508. doi: 10.1097/00004647-200405000-00003.
8. Powers WJ, Grubb RL Jr, Darriet D, Raichle ME. Cerebral blood flow and cerebral metabolic rate of oxygen requirements for cerebral function and viability in humans. *J Cereb Blood Flow Metab*. 1985;5:600–608. doi: 10.1038/jcbfm.1985.89.
9. Touzani O, Young AR, Derlon JM, Baron JC, MacKenzie ET. Progressive impairment of brain oxidative metabolism reversed by reperfusion following middle cerebral artery occlusion in anaesthetized baboons. *Brain Res*. 1997;767:17–25.
10. Touzani O, Young AR, Derlon JM, Beaudouin V, Marchal G, Rioux P, et al. Sequential studies of severely hypometabolic tissue volumes after permanent middle cerebral artery occlusion. A positron emission tomographic investigation in anesthetized baboons. *Stroke*. 1995;26:2112–2119.
11. Baron JC, Bouser MG, Lebrun-Grandie P, Iba-Zizen MT, Chiras J. Local CBF, oxygen extraction fraction (OEF), and CMRO2: Prognostic value in recent supratentorial infarction in humans. *J Cereb Blood Flow Metab*. 1983;3:S1–S2.
12. Baron JC, Marchal G. How time dependent is the threshold for cerebral infarction? *Stroke*. 1996;27:1918–1919
13. Davis SM, Donnan GA, Parsons MW, Levi C, Butcher KS, Peeters A, et al; EPITHET Investigators. Effects of alteplase beyond 3 h after stroke in the Echoplanar Imaging Thrombolytic Evaluation Trial (EPITHET): a placebo-controlled randomised trial. *Lancet Neurol*. 2008;7:299–309. doi: 10.1016/S1474-4422(08)70044-9.
14. Hacke W, Furlan AJ, Al-Rawi Y, Davalos A, Fiebach JB, Gruber F, et al. Intravenous desmoteplase in patients with acute ischaemic stroke selected by MRI perfusion-diffusion weighted imaging or perfusion CT (DIAS-2): a prospective, randomised, double-blind, placebo-controlled study. *Lancet Neurol*. 2009;8:141–150. doi: 10.1016/S1474-4422(08)70267-9.
15. Furlan AJ, Eyding D, Albers GW, Al-Rawi Y, Lees KR, Rowley HA, et al; DEDAS Investigators. Dose Escalation of Desmoteplase for Acute Ischemic Stroke (DEDAS): evidence of safety and efficacy 3 to 9 hours after stroke onset. *Stroke*. 2006;37:1227–1231. doi: 10.1161/01.STR.0000217403.66996.6d.
16. Jensen-Kondering U, Baron JC. Oxygen imaging by MRI: can blood oxygen level-dependent imaging depict the ischemic penumbra? *Stroke*. 2012;43:2264–2269. doi: 10.1161/STROKEAHA.111.632455.
17. An H, Liu Q, Chen Y, Lin W. Evaluation of MR-derived cerebral oxygen metabolic index in experimental hyperoxic hypercapnia, hypoxia, and ischemia. *Stroke*. 2009;40:2165–2172. doi: 10.1161/STROKEAHA.108.540864.
18. Heiss WD. Experimental evidence of ischemic thresholds and functional recovery. *Stroke*. 1992;23:1668–1672.
19. Furlan A, Higashida R, Wechsler L, Gent M, Rowley H, Kase C, et al. Intra-arterial prourokinase for acute ischemic stroke. The PROACT II study: a randomized controlled trial. Prolyse in Acute Cerebral Thromboembolism. *JAMA*. 1999;282:2003–2011.
20. Powers WJ. Thromobolysis for acute ischemic stroke: is intra-arterial better than intravenous? A treatment effects model. *J Stroke Cerebrovasc Dis*. 2012;21:401–403. doi: 10.1016/j.jstrokecerebrovasdis.2012.03.003.
21. Chemmanam T, Campbell BC, Christensen S, Nagakane Y, Desmond PM, Bladin CF, et al; EPITHET Investigators. Ischemic diffusion lesion reversal is uncommon and rarely alters perfusion-diffusion mismatch. *Neurology*. 2010;75:1040–1047. doi: 10.1212/WNL.0b013e3181f39ab6.
22. Gaudinski MR, Henning EC, Miracle A, Luby M, Warach S, Latour LL. Establishing final infarct volume: stroke lesion evolution past 30 days is insignificant. *Stroke*. 2008;39:2765–2768. doi: 10.1161/STROKEAHA.107.512269.
23. Wu O, Østergaard L, Weisskoff RM, Benner T, Rosen BR, Sorensen AG. Tracer arrival timing-insensitive technique for estimating flow in MR perfusion-weighted imaging using singular value decomposition with a block-circulant deconvolution matrix. *Magn Reson Med*. 2003;50:164–174. doi: 10.1002/mrm.10522.
24. An H, Lin W. Impact of intravascular signal on quantitative measures of cerebral oxygen extraction and blood volume under normo- and hypercapnic conditions using an asymmetric spin echo approach. *Magn Reson Med*. 2003;50:708–716. doi: 10.1002/mrm.10576.

25. Lee JM, Vo KD, An H, Celik A, Lee Y, Hsu CY, et al. Magnetic resonance cerebral metabolic rate of oxygen utilization in hyperacute stroke patients. *Ann Neurol*. 2003;53:227–232. doi: 10.1002/ana.10433.
26. Jenkinson M, Smith S. A global optimisation method for robust affine registration of brain images. *Med Image Anal*. 2001;5:143–156.
27. Yushkevich PA, Piven J, Hazlett HC, Smith RG, Ho S, Gee JC, et al. User-guided 3D active contour segmentation of anatomical structures: significantly improved efficiency and reliability. *Neuroimage*. 2006;31:1116–1128. doi: 10.1016/j.neuroimage.2006.01.015.
28. Warach S, Al-Rawi Y, Furlan AJ, Fiebach JB, Wintermark M, Lindstén A, et al. Refinement of the magnetic resonance diffusion-perfusion mismatch concept for thrombolytic patient selection: insights from the desmoteplase in acute stroke trials. *Stroke*. 2012;43:2313–2318. doi: 10.1161/STROKEAHA.111.642348.
29. Zazulia AR, Markam J, Powers WJ. Cerebral blood flow and metabolism in human cerebrovascular disease. In: Mohr JP, Wolf PA, eds. *Stroke: Pathophysiology, Diagnosis, and Management*. Philadelphia, PA: Elsevier Saunders; 2011:44–67.
30. Ambroise C, McLachlan GJ. Selection bias in gene extraction on the basis of microarray gene-expression data. *Proc Natl Acad Sci U S A*. 2002;99:6562–6566. doi: 10.1073/pnas.102102699.
31. Khatri P, Abruzzo T, Yeatts SD, Nichols C, Broderick JP, Tomsick TA; IMS I and II Investigators. Good clinical outcome after ischemic stroke with successful revascularization is time-dependent. *Neurology*. 2009;73:1066–1072. doi: 10.1212/WNL.0b013e3181b9c847.
32. Nagakane Y, Christensen S, Brekenfeld C, Ma H, Churilov L, Parsons MW, et al; EPITHET Investigators. EPITHET: Positive Result After Reanalysis Using Baseline Diffusion-Weighted Imaging/Perfusion-Weighted Imaging Co-Registration. *Stroke*. 2011;42:59–64. doi: 10.1161/STROKEAHA.110.580464.
33. Albers GW, Thijs VN, Wechsler L, Kemp S, Schlaug G, Skalabrin E, et al; DEFUSE Investigators. Magnetic resonance imaging profiles predict clinical response to early reperfusion: the diffusion and perfusion imaging evaluation for understanding stroke evolution (DEFUSE) study. *Ann Neurol*. 2006;60:508–517. doi: 10.1002/ana.20976.
34. Lansberg MG, Straka M, Kemp S, Mlynash M, Wechsler LR, Jovin TG, et al.; DEFUSE 2 Study Investigators. MRI profile and response to endovascular reperfusion after stroke (DEFUSE 2): a prospective cohort study. *Lancet Neurol*. 2012;11:860–867. doi: 10.1016/S1474-4422(12)70203-X.
35. Zaro-Weber O, Moeller-Hartmann W, Heiss WD, Sobesky J. MRI perfusion maps in acute stroke validated with 15O-water positron emission tomography. *Stroke*. 2010;41:443–449. doi: 10.1161/STROKEAHA.109.569889.
36. Takasawa M, Jones PS, Guadagno JV, Christensen S, Fryer TD, Harding S, et al. How reliable is perfusion MR in acute stroke? Validation and determination of the penumbra threshold against quantitative PET. *Stroke*. 2008;39:870–877. doi: 10.1161/STROKEAHA.107.500090.
37. Kidwell CS, Wintermark M, De Silva DA, Schaewe TJ, Jahan R, Starkman S, et al. Multiparametric MRI and CT models of infarct core and favorable penumbral imaging patterns in acute ischemic stroke. *Stroke*. 2013;44:73–79. doi: 10.1161/STROKEAHA.112.670034.
38. Lansberg MG, Lee J, Christensen S, Straka M, De Silva DA, Mlynash M, et al. RAPID automated patient selection for reperfusion therapy: a pooled analysis of the Echoplanar Imaging Thrombolytic Evaluation Trial (EPITHET) and the Diffusion and Perfusion Imaging Evaluation for Understanding Stroke Evolution (DEFUSE) Study. *Stroke*. 2011;42:1608–1614. doi: 10.1161/STROKEAHA.110.609008.

American Heart Association | American Stroke Association

Stroke

Defining the Ischemic Penumbra Using Magnetic Resonance Oxygen Metabolic Index

Hongyu An, Andria L. Ford, Yasheng Chen, Hongtu Zhu, Rosana Ponisio, Gyanendra Kumar, Amirali Modir Shanechi, Naim Khoury, Katie D. Vo, Jennifer Williams, Colin P. Derdeyn, Michael N. Diringer, Peter Panagos, William J. Powers, Jin-Moo Lee and Weili Lin

Stroke. published online February 26, 2015;
Stroke is published by the American Heart Association, 7272 Greenville Avenue, Dallas, TX 75231

Print ISSN: 0039-2499. Online ISSN: 1524-4628